Research Paper

Refinement by integration: aggregated effects of multimodal imaging markers on adult ADHD

Thomas Wolfers, MSc; Alberto Llera Arenas, PhD; A. Marten H. Onnink, PhD; Janneke Dammers, MSc; Martine Hoogman, PhD; Marcel P. Zwiers, PhD; Jan K. Buitelaar, MD, PhD; Barbara Franke, PhD; Andre F. Marquand, PhD; Christian F. Beckmann, PhD

Early-released on Aug. 23, 2017; subject to revision

Background: Attention-deficit/hyperactivity disorder (ADHD) is biologically heterogeneous, with different biological predispositions — mediated through developmental processes — converging upon a common clinical phenotype. Brain imaging studies have variably shown altered brain structure, activity and connectivity in children and adults with ADHD. Recent methodological developments allow for the integration of information across imaging modalities, potentially yielding a more coherent view regarding the biology underlying the disorder. **Methods:** We analyzed a sample of adults with persistent ADHD and healthy controls using an advanced multimodal linked independent component analysis approach. Diffusion and structural MRI data were fused to form imaging markers reflecting independent components that explain variation across modalities. We included these markers as predictors into logistic regression models on adult ADHD and put those into context with predictions of estimated intelligence, age and sex. **Results:** We included 87 adults with ADHD and 93 controls in our analysis. Participants' courses associated with all imaging markers explained 27.86% of the variance in adult ADHD. No single imaging modality dominated this result. Instead, it was explained by aggregation of relatively small effects across several modalities and markers. One of the top markers for adult ADHD was multimodal and linked to morphological and microstructural effects within anterior temporal brain regions; another was linked to cortical thickness. Several markers were also influenced by estimated intelligence, age and/or sex. **Limitations:** Although complex analytical approaches, such as the one applied here, provide insight into otherwise hidden mechanisms, they also increase the complexity of interpretations. **Conclusion:** No dominant imaging modality or marker characterizes structural brain phenotypes in adults with ADHD, but we can refine our characterization of the disorder by the integration of small effects across modalities.

Introduction

Attention-deficit/hyperactivity disorder (ADHD) is often perceived as a childhood disorder; however, it affects adults as well.[1,2] The prevalence of ADHD in the adult population is about 2.5%.[1] It is biologically heterogeneous,[3] suggesting that different biological predispositions — mediated through developmental processes — converge upon a common clinical phenotype.[4–9] The different mechanisms that have been proposed for ADHD[3] may be reflected to varying degrees across neuroimaging modalities.[10–16] Imaging modalities are sensitive to different properties of the underlying biological tissue. Although structural imaging captures basic tissues, such as grey and white matter volumes, diffusion imaging allows for the estimation of white matter microstructural integrity. Therefore, it is beneficial to integrate effects across a range of imaging modalities using a principled approach to refine our understanding of the biology underlying adult ADHD.

Recent methodological developments allow for this integration[17–19] and have presented novel imaging markers underlying age-dependent brain changes[17,20] or childhood and adolescent ADHD.[21] In those studies, linked independent component analysis (ICA) was used, which, in contrast to other methods, combines information already at an early stage in the analysis pipeline. This allows for a principled integration of information rather than a post hoc combination of unimodal results at the stage of final interpretation. Linked ICA searches for hidden sources of spatial variation across multiple brain imaging modalities, yielding independent components or imaging markers. Given the presumed heterogeneity of adult ADHD in terms of its biology and pathophysiological mechanisms,[3] integrating information across

Correspondence to: T. Wolfers, Donders Centre for Cognitive Neuroimaging, Radboud University, PO Box 9101, 6500 HB Nijmegen, The Netherlands; t.wolfers@donders.ru.nl

Submitted Dec. 16, 2016; Revised Apri; 13, 2017; Accepted May 10, 2017.

DOI 10.1503/jpn.160240

© 2017 Joule Inc. or its licensors

imaging modalities may yield a more complete picture of each underlying mechanism and allow for multiple mechanisms to be taken into account simultaneously.

In the present study, we took an integrative perspective on adult ADHD, combining imaging modalities into markers using a multimodal linked ICA of diffusion and structural MRI data. We integrated the resulting imaging markers using multiple logistic and linear regressions. Hypothesizing that a biologically heterogeneous phenotype, such as adult ADHD, affects different modalities at once, we expected that through such integration, a sizable and robust effect would be detectable. We contrasted the analyses with effects of estimated intelligence, age and sex to increase our understanding of the known roles of these factors on brain structure as well as ADHD and to quantify the overall magnitude of ADHD-related effects in association with these factors.

Methods

Participants

We selected adults with ADHD and healthy controls from the Dutch cohort of the International Multicentre persistent ADHD CollaboraTion[1,22] based on data availability across imaging modalities. Adults with ADHD were recruited from the Department of Psychiatry of the Radboud University Medical Centre and through advertisements. In this recruitment process, the adults with ADHD were matched for sex, age and estimated intelligence to a healthy control population. All participants underwent psychiatric assessments, neuropsychological testing, and neuroimaging. The Diagnostic Interview for Adult ADHD (DIVA)[23] was conducted to confirm the diagnosis of adult ADHD. This interview focuses on the 18 DSM-IV symptoms of ADHD and uses concrete and realistic examples to thoroughly investigate whether a symptom is currently present and whether it was already present in childhood.[24] In all cases, a childhood history of ADHD symptoms was established, and persistent ADHD was diagnosed. The ADHD Rating Scale-IV was filled in by each participant to report current symptoms of attention and hyperactivity/impulsivity. To assess comorbidities, the Structured Clinical Interviews for DSM-IV (SCID-I and SCID-II) were administered.[25–27] The inclusion criteria for participants with ADHD were DSM-IV-TR criteria for ADHD in childhood as well as in adulthood, no psychosis, no alcohol or substance addiction in the last 6 months, full-scale intelligence estimate above 70 (prorated from the Block Design and Vocabulary subtests of the Wechsler Adult Intelligence Scale-III), no neurologic disorders, no obvious sensorimotor disabilities, and no medication use other than psychostimulants or atomoxetine. Additional criteria for healthy controls were no current neurologic or psychiatric disorder according to DIVA, SCID-I, or SCID-II, and no first-degree relatives with ADHD or another major psychiatric disorder. All participants were Dutch and of European Caucasian ancestry. The regional ethics committee (Centrale Commissie Mensgebonden Onderzoek: CMO Regio Arnhem – Nijmegen) approved our study protocol. We obtained written informed consent from all participants. An overlapping sample was used earlier in unimodal analyses.[28–30]

MRI acquisition

Whole brain imaging was performed using a 1.5 T scanner (Magnetom Avanto, Siemens Medical Systems) with a standard 8-channel head coil. A high-resolution T_1-weighted magnetization-prepared rapid-acquisition gradient echo (MPRAGE) anatomic scan was obtained from each participant, in which the inversion time (TI) was chosen to provide optimal grey matter–white matter T_1 contrast (repetition time [TR] 2730 ms, echo time [TE] 2.95 ms, TI 1000 ms, flip angle 7°, field of view [FOV] $256 \times 256 \times 176$ mm^3, voxel size $1.0 \times 1.0 \times 1.0$ mm^3). The T_1 images served as a basis for the extraction of grey matter volumes, pial surface area and cortical thickness. Further, they served as high-resolution reference images for diffusion imaging data. Transversely oriented diffusion-weighted images were acquired using a twice-refocused spin echo planar imaging sequence that minimized imaging distortions from eddy currents.[31] The diffusion imaging data were acquired using 2 different protocols. Forty participants were scanned with the following protocol: TR 10 200 ms, TE 95 ms, FOV $320 \times 320 \times 160$ mm^3, voxel size $2.5 \times 2.5 \times 2.5$ mm^3, 6/8 partial Fourier acquisition. Four images without diffusion weighting (b = 0 s/mm^2) and 30 images with diffusion weighting (b = 900 s/mm^2) applied along evenly distributed directions were acquired. The remaining 140 participants were scanned with an adapted second protocol, which was implemented to reduce motion artifacts during scanning. Parameters that differed from the first protocol were TR (6700 ms), TE (85 ms), FOV ($220 \times 220 \times 140$ mm^3), and full Fourier acquisition; other parameters were unchanged. Imaging markers that were significantly affected by a difference in scan protocol were excluded from statistical analyses.

MRI processing

Diffusion parameters

Preprocessing of diffusion MRI scans entailed denoising,[32] realignment, residual eddy-current correction (SPM8), artifact removal from head and/or cardiac motion (PATCH) and correction for magnetic susceptibility-induced distortions.[34] The preprocessed diffusion data were fed into FSL version 4.1.7,[35] and diffusion tensor model fit was used to derive fractional anisotropy (FA), mean diffusivity (MD), and tensor mode (MO) at each voxel.[36] These measures in principle quantify the shape of the diffusion tensor[37] (i.e., FA measures the anisotropy of diffusion, MD measures the overall magnitude of diffusion, and MO reflects the shape of the diffusion tensor). These measures were fed into the tract-based spatial statistics (FSL-TBSS) pipeline for skeletonization[38] and nonlinearly registered to the FMRIB-58_FA template (Montreal Neurological Institute [MNI]152 space). The skeleton was thresholded at FA ≥ 0.2, and its resolution was reduced from 1 mm to 2 mm isotropic voxel size for computational reasons.

Cortical thickness and areal expansion

Structural MRI images were fed into FreeSurfer software version 5.3 to extract measures for cortical thickness and areal expansion (http://surfer.nmr.mgh.harvard.edu/).[39,40] The standard FreeSurfer preprocessing pipeline (recon-all) was applied to these images, in which a reconstruction of the cortical sheet was estimated using intensity and continuity information. Cortical thickness was determined as the closest distance from the grey matter/white matter boundary to the grey matter/cerebrospinal fluid (CSF) boundary at each vertex.[41] Surface area in FreeSurfer is estimated as the relative amount of expansion or compression at each vertex when registering each participant's surface to a common atlas. Surface maps were resampled and mapped to a common coordinate system.[42] During preprocessing, the data were registered onto the high-resolution average participant surface space (fsaverage), and a 10 mm full-width at half-maximum (FWHM) surface-based smoothing kernel was applied.

Grey matter volume

Prior to grey matter volume estimation, all participants' T_1 images were rigidly aligned using statistical parametric mapping version 12 (SPM-12). Subsequently, images were segmented, normalized, and bias field–corrected using "new segment" from VBM-SPM12 (www.fil.ion.ucl.ac.uk/spm),[43,44] yielding images containing grey and white matter segments plus CSF. We then used DARTEL[45] to create a study-specific grey matter template to which all segmented images were normalized. Subsequently, all grey matter volumes were smoothed with a 9.4 mm FWHM Gaussian smoothing kernel (corresponding to $\sigma = 4$ mm). Data were downsampled from 2 mm to 4 mm isotropic resolution for computational reasons.

Linked ICA

Linked ICA[18] is a Bayesian spatial multimodal extension of the common ICA model.[46,47] Whereas most ICA algorithms perform factorization of time-series, the linked ICA algorithm provides a factorization over participants. This model can simultaneously decompose data modalities, with different numbers of features, while ensuring balance of information across modalities. Each of the linked ICA components is linked to a participant course (1 scalar value per participant) and each modality's corresponding spatial map.[48] The participant courses can be analyzed in association with behavioural measures, explaining, for example, development, behaviour, or pathologies. Here, linked ICA was used to combine 6 data modalities: FA, MD, MO, cortical thickness, areal expansion estimates and grey matter volume. We decided to estimate 50 independent components, following recommendations described in earlier papers.[17,18,21] It would have been justifiable to use 40–50 imaging markers based on these recommendations. Therefore, we repeated the ICA model estimations using 40 and 45 imaging markers. We used the code available on the FSL homepage,[2] and for further discussions of the method, we referred to the original papers.[17,18] For visualization, the spatial maps were converted to pseudo-Z-statistics and thresholded at $|Z| > 2.3$. Throughout the text, we refer to the independent components derived from linked ICA analysis as imaging markers or simply markers. If a marker was associated with multiple data modalities, we called it a multimodal marker. Statistical inferences were performed on the associated participants' courses.

Statistical analysis

Prior to statistical inference, 13 imaging markers were excluded from further analyses, as they were either dominated by a single participant (i.e., more than 10% of the variance was explained by a single participant) or they were associated with the diffusion acquisition protocol (Appendix 1, Table S1, available at jpn.ca). Thus, we analyzed a total of 37 imaging markers in our main analyses.

Complex and heterogeneous phenotypes, such as adult ADHD, are unlikely to be affected by a single imaging marker in isolation. Therefore, we performed a descriptive logistic regression analysis on adult ADHD with the participants' loadings associated with the 37 imaging markers as regressors. We compared this descriptive logistic regression model to 3 other models containing the same regressors but different criteria, namely, sex, age and estimated intelligence. We report only the results that remained significant after multiple comparison corrections using the Bonferroni–Holm method[49] (significance level of $p < 0.05/4$) and interpreted only individual regressors (imaging markers) that remained significant after correcting for the total number of regressors in an overall significant regression model using the Bonferroni–Holm method (significance level of $p < 0.05/37$). The 2 thresholds were determined based on the number of independent regressions (adult ADHD, estimated intelligence, age and sex) or the number of predictors in each individual model (37 imaging markers).

We performed a number of sensitivity analyses to determine the specificity, robustness and generalizability of our main results. To increase the confidence in the specificity of our findings, we controlled for sex, age and estimated intelligence in a separate model of adult ADHD. Further, we correlated self-reported symptoms of inattention and hyperactivity/impulsivity with the top imaging markers associated with adult ADHD across and within each group. We tested the robustness of our results by repeating the main analyses using 40 and 45 imaging markers that were the result of a re-estimated linked ICA decomposition. We correlated the top markers associated with adult ADHD across these ICA decompositions to show their similarity. To determine if the results were linked to the selection of participants, we split each group in our sample into 2 parts based on odd and even participant numbers. We repeated the analyses in each of these splits and compared the outcomes. We estimated the generalizability of the results by determining the out-of-sample performance of the logistic regression model on adult ADHD using a "leave 1 participant out" cross-validation procedure. Here, we estimated significance using permutation testing with 1000 permutations.

In independent analyses, we performed 4 logistic regressions on adult ADHD. In those analyses, we included the top 10% of the markers, which were associated with adult ADHD, estimated intelligence, age and sex as regressors. In this way, we tested the exploratory value of imaging markers primarily associated with age, sex and estimated intelligence, for adult ADHD. All analyses were performed using StatsModels in Python.[3]

Results

Participants

We included 87 adults with ADHD and 93 healthy controls in our analyses. The demographic and clinical characteristics of the sample are shown in Table 1.

Imaging markers primarily linked to adult ADHD

Figure 1 depicts all imaging makers that were included into the descriptive regression analysis on adult ADHD. The markers were ranked based on their contribution to the model. Participants' courses associated with all imaging markers explained 27.86% of the variance in adult ADHD (Table 2). Note that this measure reflects the within-sample explained variance. Using the "leave 1 participant out" cross-validation procedure in a predictive regression analysis, we could significantly predict adult ADHD with an accuracy of 60% (p = 0.006). For a full overview of the model, refer to Appendix 1, Table S2. The sensitivity analysis including estimated intelligence, age and sex on top of the imaging markers supported the specificity of our findings for adult ADHD (Appendix 1,

Table 1: Demographics and clinical characteristics of study participants (n = 180)

Characteristic	Group; % or mean ± SD		
	Adult ADHD* (n = 87)	Control (n = 93)	p value
Male sex	31.0	29.0	—
Diffusion protocol 1	71.3	83.8	—
Age, yr	32.9 ± 9.5	35.1 ± 11.7	0.18
Estimated intelligence†	109.4 ± 15.9	107.8 ± 14.9	0.47
Hyp/imp symptoms‡	5.54 ± 2.4	0.95 ± 1.4	< 0.001
Inattention symptoms§	6.5 ± 2.0	0.6 ± 1.1	< 0.001
Comorbid disorders¶	1.31 ± 1.3	0.28 ± 0.6	< 0.001

ADHD = attention-deficit/hyperactivity disorder; hyp/imp = hyperactivity/impulsivity; SD = standard deviation.
*Diagnosis was based on the structured Diagnostic Interview for ADHD in Adults.
†Estimated intelligence was based on the Block-design and Vocabulary subtests of the Wechsler Adult Intelligence Scale.
‡Self-reported number of hyperactivity/impulsivity symptoms, as measured with the ADHD-DSM-IV rating scale.
§Self-reported number of inattention symptoms, as measured with the ADHD-DSM-IV rating scale.
¶Number of comorbid disorders, such as major depressive disorder, based on the Structured Clinical Interview.

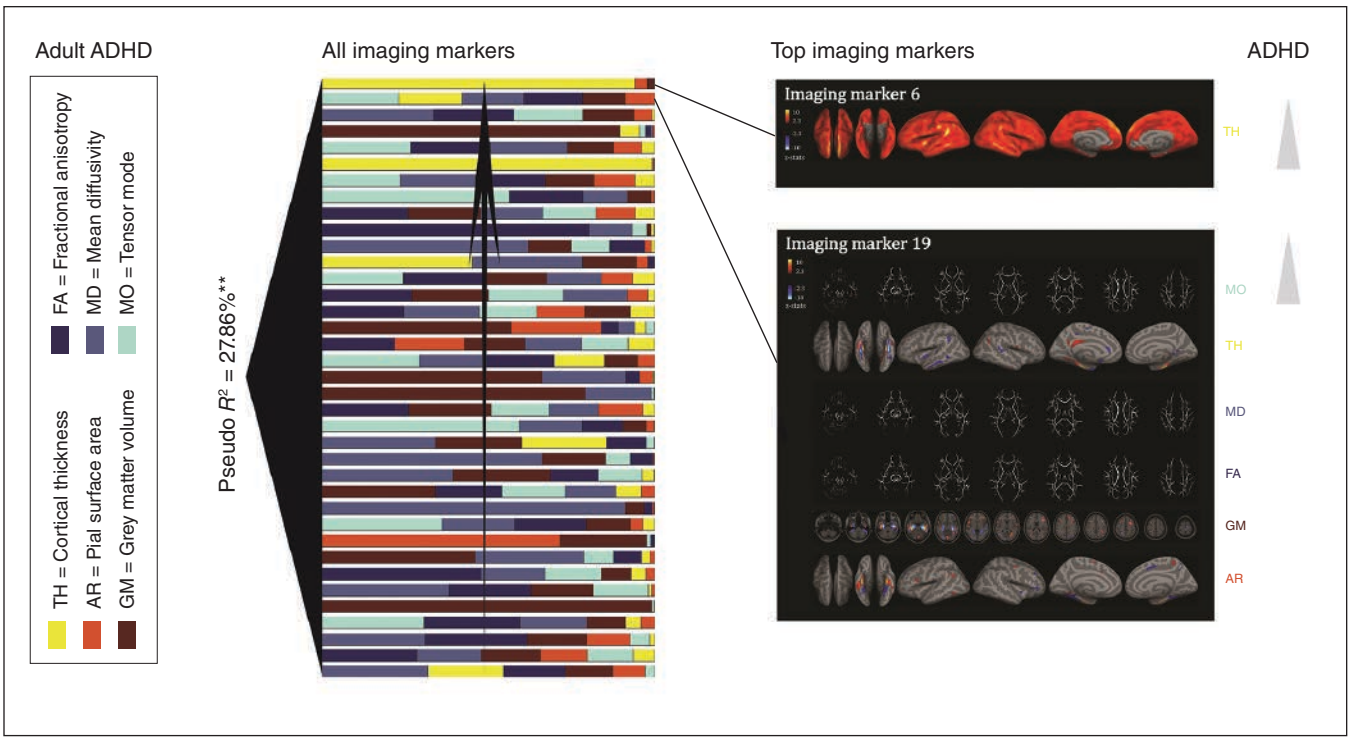

Fig. 1: All imaging markers associated with adult attention-deficit/hyperactivity disorder (ADHD) are depicted. These markers are ranked based on their contributions to the descriptive logistic regression model. Toward the left of each figure the pseudo R^2 across all imaging markers is depicted. The spatial patterns are depicted for the top 2 imaging markers associated with adult ADHD, as they remained significant after within-model correction for multiple comparisons. AR = pial surface area; FA = fractional anisotropy; GM = grey matter volume; MD = mean diffusivity; MO = tensor mode; TH = cortical thickness. **Effects that remained significant after multiple comparison correction (p < 0.05/4).

Table S3). To further increase the confidence in our results, we repeated the analysis on adult ADHD using the 50 original markers as well as models based on 40 and 45 imaging markers. In all cases the main results remained robust (Appendix 1, Table S4 and Table S5). We correlated the top markers of these different ICA models and showed that they correlated almost perfectly, thus our results remain robust regardless of the number of prespecified ICA decompositions (Appendix 1, Table S5). Additionally, we split our sample in 2 subgroups (odd- and even-number participants) and estimated logistic regressions in each of these subgroups separately, using only markers that were at least nominally significant in the original model. We could show that the regressions remained significant in both groups (Appendix 1, Table S6).

Imaging markers 6 and 19 contributed significantly to the logistic regression model on adult ADHD (Table 1) and remained at least nominally significant during various sensitivity analyses. Marker 6 was unimodal, showing contributions of cortical thickness across the whole cortex. Marker 19 was multimodal, with strong contributions from the temporal pole, parahippocampal gyrus, occipitotemporal gyrus, inferior temporal gyrus and hippocampal complex (Fig. 1). Both markers associated positively with adult ADHD. In a sensitivity analysis, we could show that neither of these markers was associated with self-reported symptoms of hyperactivity/impulsivity nor with symptoms of inattention in the individual groups; however, when combining the adult ADHD and healthy control groups to perform the same correlation analysis, inattention was associated with both markers, whereas hyperactivity/impulsivity was associated only with marker 19 (Appendix 1, Fig. S2).

Estimated intelligence, age and sex in the context of adult ADHD

Figure 2 depicts imaging markers associated with adult ADHD, estimated intelligence, age and sex. Comparable to adult ADHD, all imaging markers explained 32.21% of the variance in estimated intelligence (Appendix 1, Table S7), 78.82% of the variance in age (Appendix 1, Table S8) and 57.51% of the variance in sex (Appendix 1, Table S9). The logistic regression analyses on adult ADHD using the 10% most predictive imaging markers for estimated intelligence, age and sex explained 5.11%, 3.87% and 0.86% of the variance in adult ADHD, respectively (Table 3). In contrast, the top 10% of the imaging markers associated with adult ADHD explained 8.94% of the variance in adult ADHD. Whereas markers primarily linked to estimated intelligence and age were associated with adult ADHD, markers primarily linked to sex were not.

Discussion

In the present study, we took an integrative perspective on adult ADHD, combining different neuroimaging modalities into imaging markers using a data-driven multivariate analysis method. Imaging markers explained 27.86% of the within-sample variance in adult ADHD, which was comparable to estimated intelligence. This translated to a cross-validated accuracy of 60.00%. Both adult ADHD and estimated intelligence were associated with multiple markers across different modalities, with relatively small contributions to the descriptive regression models. Among the top 2 markers with the strongest predictive value for adult ADHD, one was unimodal, predominantly affected by cortical thickness, and widespread, and the other was bilateral and multimodal, with focal effects localized predominantly to temporal brain regions. In general, adult ADHD was associated with heterogeneous effects across markers. The markers with the strongest association with estimated intelligence and age showed a link to adult ADHD. Markers prominently linked to sex did not.

Individual imaging markers showed a weaker association with adult ADHD, but their combination was predictive. This result may speak to the heterogeneity of ADHD and supports the model that divergent brain mechanisms — evident to varying degrees in different neuroimaging modalities — converge

Table 2: Logistic regression analysis of adult ADHD (*n* = 180)

Analysis	Regression coefficient	Statistical test	Accuracy	*p* value
Descriptive logistic regression*	—	R^2_{36} = 27.86%	75.50%	0.004‡
Predictive logistic regression†			60.00%	< 0.001‡§
Individual markers				
M6	0.76	z = 3.24		0.001‡
M19	0.70	z = 3.26		0.001‡
M32	0.51	z = 2.26		0.024
M1	–0.54	z = –2.2		0.028
M38	–0.45	z = –2.17		0.030
M47	–0.50	z = –1.96		0.049

ADHD = attention-deficit/hyperactivity disorder; Permutation p = p-value using permutation testing.
*Degrees of freedom residuals = 143.
†Leave 1 participant out cross-validation method.
‡Overall regression model that remained significant after multiple comparisons using the Bonferroni–Holm method ($p < 0.05/4$) or an individual regressor that remained significant after multiple comparison correction ($p < 0.05/37$). The thresholds were determined based on the number of independent regressions (adult ADHD, estimated intelligence, age and sex) or the number of predictors in each individual model (37 imaging markers).
§Derived using permutation testing.

toward the same clinical phenotype in different adults with ADHD. Alternatively, the present results may be interpreted in such a way that multiple imaging markers may in combination be less prone to noise or capture different aspects of biology that better link to biological reality. Similar to the way that distance from downtown and square footage interactively predict property values in city centres, different independent imaging markers in combination may better explain complex phenotypes, such as adult ADHD. Our results are in line with this hypothesis and therefore support integration as a means to extend our understanding of adult ADHD.

The imaging markers that contributed most to the regression model on adult ADHD suggest that cortical thickness across the whole cortex as well as multimodal effects in anterior temporal brain regions are most predictive of adult ADHD. Adult ADHD is associated with all imaging modalities[13,21,50,51] both within and across markers (Fig. 1). One of the 2 markers prominently linked to adult ADHD, imaging

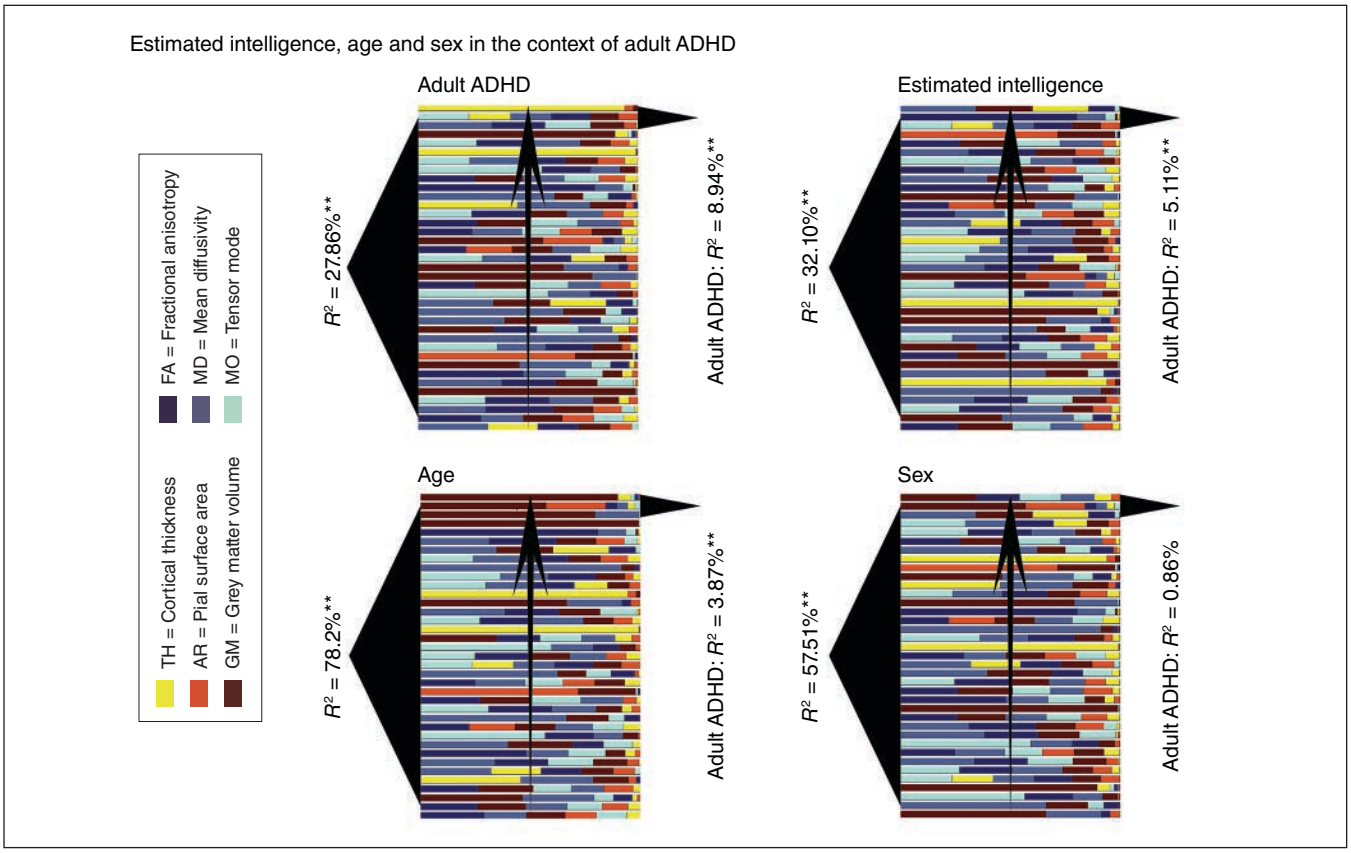

Fig. 2: Imaging markers associated with adult ADHD, estimated intelligence, age and sex. All markers are ranked based on their contribution to the respective regression. To the left of each subfigure R^2 in relation to adult ADHD, estimated intelligence, age and sex are depicted. To the right of each figure, R^2 in relation to adult ADHD for the top 10% of the markers associated with adult ADHD, estimated intelligence, age and sex are depicted. Note that the top markers for estimated intelligence and age are in this order predictive for adult ADHD, but the top markers for sex are not. These findings suggest shared brain substrates for estimated intelligence and adult ADHD as well as age and adult ADHD. AR = pial surface area; FA = fractional anisotropy; GM = grey matter volume; MD = mean diffusivity; MO = tensor mode; TH = cortical thickness. **Effects that remained significant after multiple comparison correction ($p < 0.05/4$).

Table 3: Top imaging marker logistic regressions

	Analysis; top 10% imaging markers			
Predictor	Adult ADHD (M6, M19, M32)	Estimated intelligence* (M35, M4, M19)	Age (M1, M3, M8)	Sex (M34, M3, M35)
Criterion	Adult ADHD	Adult ADHD	Adult ADHD	Adult ADHD
Pseudo R^2	8.95%	5.11%	3.87%	0.86%
p value	< 0.001†	0.001†	0.007†	0.65

ADHD = attention-deficit/hyperactivity disorder; M = imaging marker.
*Estimated intelligence was based on the Block-design and Vocabulary subtests of the Wechsler Adult Intelligence Scale.
†Overall regression model significant after Bonferroni–Holm correction ($p < 0.05/4$).

marker 19, was multimodal. The marker showed a focal pattern, with effects primarily in bilateral areas of the temporal pole, parahippocampal gyrus, occipitotemporal gyrus, inferior temporal gyrus and hippocampal complex. Differences in ADHD cohorts have been reported in the temporal pole.[7,9,52,53] However, findings have varied, and other brain regions were reported more frequently in the literature.[3,7,11,12,50,54] In a recent large meta-analysis of functional MRI studies in adults with ADHD, the left temporal pole was among the regions showing greater activation in controls than in participants with ADHD.[55] The present results suggest a complex pattern with focal effects on grey matter volume, surface and thickness as well as white matter integrity in anterior temporal brain regions.

The top 10% of the markers that showed the strongest association with estimated intelligence as well as age were also predictive of adult ADHD. Children and adults with ADHD have on average a lower intelligence than healthy individuals, and the disorder is linked to development.[3,6,56–58] However, shared brain mechanisms of those phenotypes remain to be found. Although studies have shown a genetic overlap between ADHD and low intelligence,[59] the corresponding brain substrates have not been reported. In the present study, we showed that the top markers linking to estimated intelligence were also predictive of adult ADHD, particularly one dominated by anterior temporal brain regions (marker 19). Additionally, we showed that the top markers linked to age were also predictive of adult ADHD, highlighting the developmental character of the disorder[5,6,8,30] also in adulthood. Further, in addition to studies using only structural modalities,[17,20] our results suggest that aging manifested itself best in grey matter volume rather than in, for example, diffusion measures. Therefore, grey matter volume may be a better readout to identify developmental effects in adult participants with ADHD rather than other modalities. Surprisingly, the top imaging markers associated with sex were not predictive of adult ADHD, indicating that a higher prevalence of men with ADHD is not explained by sex differences in brain morphology. Altogether, the present results point to a common substrate for intelligence and adult ADHD in multimodal imaging markers and for aging and adult ADHD in grey matter volume.

Although the present study is, to our knowledge, the first to use multimodal linked ICA in adult participants with ADHD, some studies in children and adolescents with the disorder already exist. One of these studies reported differences in multimodal imaging markers primarily in frontal regions across participants with ADHD.[21] That study included structural and diffusion imaging modalities. Another study, which included resting state as well as structural modalities,[60] reported that reduced segregation of default mode and task positive network activity co-occurred with structural abnormalities in the dorsolateral and anterior cingulate cortex. This finding is in line with unimodal work on childhood and adolescent ADHD.[3] As we included different modalities into our study, the present results are not directly comparable to those mentioned above. However, we did not find a strong frontal component in adult participants with ADHD. This may suggest that adults with ADHD, in comparison with healthy controls, have developed sufficient frontal control, which may result in a reduction of hyperactive/impulsive symptoms in adulthood. Further, multimodal investigation of this mechanism over development is an interesting topic for future research.

Limitations

The results presented in this article are robust, as exemplified in various sensitivity analyses; however, some limitations require attention. First, the analytical approach requires the model order or the number of imaging markers to be chosen before linked ICA decomposition. Our choice of 50 imaging markers was based on recommendations and earlier work.[17,18,61] Forty or 45 markers would have been justifiable as well. To rule out any effect that this choice had on the results, we repeated the analyses using these specifications. We were able to show that the results remained robust (Appendix 1, Table S4). Second, although complex analytical approaches, such as the one applied here, allow for insights into otherwise hidden mechanisms, they also increase the complexity of interpretations.[17,62] In our opinion, however, such analytical integration is essential for a better understanding of complex brain disorders and behavioural traits. Third, although we strictly quality-controlled our input imaging data and phenotypic data, only 37 imaging markers survived quality control. Repeating our analysis with all 50 imaging markers, however, had no significant effect on our results (Appendix 1, Table S4 and Table S5). Fourth, the "leave 1 participant out" cross-validation yielded relatively low accuracy. However, the results were well in line with earlier work on ADHD.[16,51] Importantly, our main purpose for the present study was to show that information predictive of adult ADHD is found across modalities and that a description of this disorder in terms of its biological heterogeneity[63] requires the integration of information across biological read-outs.

Conclusion

Our findings strongly suggest that small effects across modalities and imaging markers require integration to refine the characterization of adult ADHD, as no dominant modality or marker exists.

Acknowledgements: The research leading to these results has received funding from the European Community's Seventh Framework Programme (FP7/2007-2013) under grant agreement no. 602450 (IMAGEMEND). In addition, the study was supported by grants from the Netherlands Organization for Scientific Research (NWO), a Vici grant to B. Franke (grant no. 016-130-669), Brain & Cognition grants no. 433-09-242 and no. 056-13-015 to J. Buitelaar, and the Gravitation Programme Language in Interaction (grant 024.001.006). The research of B. Franke and J. Buitelaar also receives funding from the FP7 Programme under grant agreements no. 602805 (AGGRESSOTYPE), no. 603016 (MATRICS) and no. 278948 (TACTICS), from the European Community's Horizon 2020 Programme (H2020/2014–2020) under grant agreements no. 643051 (MiND) and no. 642996 (BRAINVIEW), and from a grant for the ENIGMA Center for Worldwide Medicine Imaging and Genomics from the National Institute of Health's BD2K Initiative (grant no. U54 EB020403). A. Marquand acknowledges support from the

Language in Interaction consortium, funded by the NWO under the Gravitation Programme.

Affiliations: From the Department of Human Genetics, Donders Institute for Brain, Cognition and Behaviour, Radboud University Medical Centre, Nijmegen, the Netherlands (Wolfers, Onnink, Dammers, Hoogman, Franke); the Donders Centre for Cognitive Neuroimaging, Donders Institute for Brain, Cognition and Behaviour, Radboud University, Nijmegen, the Netherlands (Wolfers, Arenas, Hoogman, Zwiers, Franke, Marquand, Beckman); the Department of Cognitive Neuroscience, Donders Institute for Brain, Cognition and Behaviour, Radboud University Medical Centre, Nijmegen, the Netherlands (Buitelaar, Marquand, Beckmann); the Centre for Functional MRI of the Brain (FMRIB), Oxford University, Oxford, UK (Beckmann); the Department of Psychiatry, Donders Institute for Brain, Cognition and Behaviour, Radboud University Medical Centre, Nijmegen, the Netherlands (Franke); the Karakter Child and Adolescent Psychiatry University Centre, Radboud University Medical Centre, Nijmegen, the Netherlands (Buitelaar); and the Department of Neuroimaging, Institute of Psychiatry, King's College London, London, UK (Marquand).

Competing interests: J. Buitelaar has been a consultant, member of the advisory board and/or speaker for Janssen Cilag BV, Eli Lilly, Shire, Lundbeck, Roche and Servier. B. Franke has received speaker fees from Merz. None of these companies or any of the funding agencies had any influence on the content of this paper. No other competing interests declared.

Contributors: T. Wolfers, A. Arenas, B. Franke, A. Marquand and C. Beckmann designed the study. T. Wolders, M. Onnink, J. Dammers, M. Hoogman, M. Zwiers, J. Buitelaar and B. Franke acquired the data, which T. Wolfers, A. Arenas, M. Zwiers, J. Buitelaar, B. Franke, A. Marquand and C. Beckmann analyzed. T. Wolfers, A. Arenas and A. Marquand wrote the article, which all authors reviewed and approved for publication.

References

1. Simon V, Czobor P, Balint S, et al. Prevalence and correlates of adult attention-deficit hyperactivity disorder: meta-analysis. *Br J Psychiatry* 2009;194:204-11.
2. Franke B, Faraone SV, Asherson P, et al. The genetics of attention deficit/hyperactivity disorder in adults, a review. *Mol Psychiatry* 2012;17:960–87.
3. Faraone SV, Asherson P, Banaschewski T, et al. Attention-deficit/hyperactivity disorder. *Nat Rev Dis Prim* 2015;1:15020.
4. Seidman LJ, Biederman J, Liang L, et al. Gray matter alterations in adults with attention-deficit/hyperactivity disorder identified by voxel based morphometry. *Biol Psychiatry* 2011;69:857–66.
5. Greven CU, Bralten J, Mennes M, et al. Developmentally stable whole-brain volume reductions and developmentally sensitive caudate and putamen volume alterations in those with attention-deficit/hyperactivity disorder and their unaffected siblings. *JAMA Psychiatry* 2015;72:490-9.
6. Shaw P, Eckstrand K, Sharp W, et al. Attention-deficit/hyperactivity disorder is characterized by a delay in cortical maturation. *Proc Natl Acad Sci U S A* 2007;104:19649–54.
7. Cortese S, Kelly C, Chabernaud C, et al. Toward systems neuroscience of ADHD: a meta-analysis of 55 fMRI studies. *Am J Psychiatry* 2012;169:1038-55.
8. Krain AL, Castellanos FX. Brain development and ADHD. *Clin Psychol Rev* 2006;26:433–44.
9. Castellanos FX, Proal E. Large-scale brain systems in ADHD: beyond the prefrontal-striatal model. *Trends Cogn Sci* 2012;16:17-26.
10. Bush G, Valera EM, Seidman LJ. Functional neuroimaging of attention-deficit/hyperactivity disorder: a review and suggested future directions. *Biol Psychiatry* 2005;57:1273-84.
11. Valera EM, Faraone SV, Murray KE, et al. Meta-analysis of structural imaging findings in attention-deficit/hyperactivity disorder. *Biol Psychiatry* 2007;61:1361-9.
12. Seidman LJ, Valera EM, Makris N. Structural brain imaging of attention-deficit/hyperactivity disorder. *Biol Psychiatry* 2005;57:1263–72.
13. van Ewijk H, Heslenfeld DJ, Zwiers MP, et al. Diffusion tensor imaging in attention deficit/hyperactivity disorder: a systematic review and meta-analysis. *Neurosci Biobehav Rev* 2012;36:1093–106.
14. Cortese S, Castellanos FX. Neuroimaging of attention-deficit/hyperactivity disorder: current neuroscience-informed perspectives for clinicians. *Curr Psychiatry Rep* 2012;14:568-78.
15. van Rooij D, Hartman CA, Mennes M, et al. Altered neural connectivity during response inhibition in adolescents with attention-deficit/hyperactivity disorder and their unaffected siblings. *Neuroimage Clin* 2015;7:325–35.
16. Wolfers T, van Rooij D, Oosterlaan J, et al. Quantifying patterns of brain activity: distinguishing unaffected siblings from participants with ADHD and healthy individuals. *Neuroimage Clin* 2016;12:227–33.
17. Groves AR, Smith SM, Fjell AM, et al. Benefits of multi-modal fusion analysis on a large-scale dataset: life-span patterns of inter-subject variability in cortical morphometry and white matter microstructure. *Neuroimage* 2012;63:365–80.
18. Groves AR, Beckmann CF, Smith SM, et al. Linked independent component analysis for multimodal data fusion. *Neuroimage* 2011; 54:2198–217.
19. Sui J, Adali T, Yu Q, et al. A review of multivariate methods for multimodal fusion of brain imaging data. *J Neurosci Methods* 2012;204:68–81.
20. Douaud G, Groves AR, Tamnes CK, et al. A common brain network links development, aging, and vulnerability to disease. *Proc Natl Acad Sci U S A* 2014;111:17648.
21. Francx W, Llera A, Mennes M, et al. Integrated analysis of gray and white matter alterations in attention-deficit/hyperactivity disorder. *NeuroImage Clin* 2016;11:357–67.
22. Hoogman M, Aarts E, Onnink M, et al. Nitric oxide synthase genotype modulation of impulsivity and ventral striatal activity in adult ADHD patients and healthy comparison subjects. *Am J Psychiatry* 2011;168:1099-106.
23. Kooij J. Diagnostic Interview for ADHD in Adults 2.0 (DIVA 2.0). Adult ADHD Diagnostic Assess Treat 2010.
24. Kooij SJJ, Boonstra MA, Swinkels SHN, et al. Reliability, validity, and utility of instruments for self-report and informant report concerning symptoms of ADHD in adult patients. *J Atten Disord* 2008;11:445–58.
25. Weertman A, Arntz A, Dreessen L, et al. Short-interval test-retest interrater reliability of the Dutch version of the Structured Clinical Interview for DSM-IV personality disorders (SCID-II). *J Pers Disord* 2003;17:562-7.
26. Van Groenestijn MAC, Akkerhuis GW, Kupka RW, et al. Gestructureerd klinisch interview voor de vaststelling van DSM-IV as-I stoornissen (SCID-I). Lisse, The Netherlands: Swets & Zeitlinger.; 1999.
27. Lobbestael J, Leurgans M, Arntz A. Inter-rater reliability of the Structured Clinical Interview for DSM-IV Axis I Disorders (SCID I) and Axis II Disorders (SCID II). *Clin Psychol Psychother* 2011;18:75-9.
28. Wolfers T, Onnink AMH, Zwiers MP, et al. Lower white matter microstructure in the superior longitudinal fasciculus is associated with increased response time variability in adults with attention-deficit/hyperactivity disorder. *J Psychiatry Neurosci* 2015;40:334-51.
29. Onnink AMH, Zwiers MP, Hoogman M, et al. Deviant white matter structure in adults with attention-deficit/hyperactivity disorder points to aberrant myelination and affects neuropsychological performance. *Prog Neuropsychopharmacology Biol Psychiatry* 2015;63:14–22.
30. Onnink AMH, Zwiers MP, Hoogman M, et al. Brain alterations in adult ADHD: effects of gender, treatment and comorbid depression. *Eur Neuropsychopharmacol* 2014;24:397–409.
31. Reese TG, Heid O, Weisskoff RM, et al. Reduction of eddy-current-induced distortion in diffusion MRI using a twice-refocused spin echo. *Magn Reson Med* 2003;49:177-82.
32. Manjón JV, Coupe P, Concha L, et al. Diffusion weighted image denoising using overcomplete local PCA. *PLoS One* 2013;8:e73021-12.
33. Zwiers MP. Patching cardiac and head motion artefacts in diffusion-weighted images. *Neuroimage* 2010;53:565–75.
34. Visser E, Qin S, Zwiers MP. EPI distrotion correction by constrained ninlinear coregistration improves group FMRI. *Jt Annu Meet* ISMRM-ESMRMB 2010;3459.
35. Jenkinson M, Beckmann CF, Behrens TEJ, et al. Fsl. *Neuroimage* 2012;62:782-90.
36. Behrens TEJ, Woolrich MW, Jenkinson M, et al. Characterization and propagation of uncertainty in diffusion-weighted MR imaging. *Magn Reson Med* 2003;50:1077-88.
37. Basser PJ, Mattiello J, LeBihan D. MR diffusion tensor spectroscopy and imaging. *Biophys J* 1994;66:259–67.

38. Smith SM, Jenkinson M, Johansen-Berg H, et al. Tract-based spatial statistics: voxelwise analysis of multi-subject diffusion data. *Neuroimage* 2006;31:1487–505.
39. Dale AM, Fischl B, Sereno MI. Cortical surface-based analysis. I. Segmentation and surface reconstruction. *Neuroimage* 1999;9:179-94.
40. Fischl B, Sereno MI, Dale AM. Cortical surface-based analysis II: inflation, flattening, and a surface-based coordinate system. *Neuroimage* 1999;9:195-207.
41. Fischl B, Dale AM. Measuring the thickness of the human cerebral cortex from magnetic resonance images. *Proc Natl Acad Sci U S A* 2000;97:11050-5.
42. Fischl B, Rajendran N, Busa E, et al. Cortical folding patterns and predicting cytoarchitecture. *Cereb Cortex* 2008;18:1973-80.
43. Ashburner J, Friston KJ. Voxel-based morphometry — the methods. *Neuroimage* 2000;11:805-21.
44. Ashburner J, Friston KJ. Unified segmentation. *Neuroimage* 2005;26:839-51.
45. Ashburner J. A fast diffeomorphic image registration algorithm. *Neuroimage* 2007;38:95-113.
46. Hyvärinen A. Fast and robust fixed-point algorithm for independent component analysis. *IEEE Trans Neural Netw* 1999;10:626-34.
47. Jutten C, Herault J. Blind seperation of sources, part I: an adaptive algorithm based on neuromimetic architecture. *Signal Process* 1991; 24:1-10.
48. Beckmann CF, Smith SM. Tensorial extensions of independent component analysis for multisubject FMRI analysis. *Neuroimage* 2005;25:294-311.
49. Holm S. A simple sequentially rejective multiple test procedure. *Statistics (Ber)* 1979;6:65–70.
50. Makris N, Biederman J, Valera EM, et al. Cortical thinning of the attention and executive function networks in adults with attention-deficit/hyperactivity disorder. *Cereb Cortex* 2007;17:1364–75.
51. Wolfers T, Buitelaar JK, Beckmann CF, et al. From estimating activation locality to predicting disorder: a review of pattern recognition for neuroimaging-based psychiatric diagnostics. *Neurosci Biobehav Rev* 2015;57:328–49.
52. Fernandez-Jaen A, Lopez-Martin S, Albert J, et al. Cortical thinning of temporal pole and orbitofrontal cortex in medication-naive children and adolescents with ADHD. *Psychiatry Res Neuroimaging* 2014;224:8–13.
53. Sasayama D, Hayashida A, Yamasue H, et al. Neuroanatomical correlates of attention-deficit-hyperactivity disorder accounting for comorbid oppositional defiant disorder and conduct disorder. *Psychiatry Clin Neurosci* 2010;64:394-402.
54. von Rhein D, Oldehinkel M, Beckmann CF, et al. Aberrant local striatal functional connectivity in attention-deficit/hyperactivity disorder. *J Child Psychol Psychiatry* 2016;57:697-705.
55. Cortese S, Castellanos FX, Eickhoff CR, et al. Archival report functional decoding and meta-analytic connectivity modeling in adult attention-deficit/hyperactivity disorder. *Biol Psychiatry* 2016;80:1–10.
56. Bridgett DJ, Walker ME. Intellectual functioning in adults with ADHD: a meta-analytic examination of full scale IQ differences between adults with and without ADHD. *Psychol Assess* 2006;18:1-14.
57. Frazier TW, Youngstrom EA, Glutting JJ, et al. ADHD and achievement: meta-analysis of the child, adolescent, and adult literatures and a concomitant study with college students. *J Learn Disabil* 2007;40:49-65.
58. Hoogman M, Bralten J, Hibar DP, et al. Subcortical brain volume differences in participants with attention deficit hyperactivity disorder in children and adults: a cross-sectional mega-analysis. *Lancet Psychiatry* 2017;4:310-9.
59. Kuntsi J, Eley TC, Taylor A, et al. Co-occurrence of ADHD and low IQ has genetic origins. *Am J Med Genet B Neuropsychiatr Genet* 2004;124B:41-7.
60. Kessler D, Angstadt M, Welsh RC, et al. Modality-spanning deficits in attention-deficit/hyperactivity disorder in functional networks, gray matter, and white matter. *J Neurosci* 2014;34:16555–66.
61. Francx W, Oldehinkel M, Oosterlaan J, et al. The executive control network and symptomatic improvement in attention-deficit/hyperactivity disorder. *Cortex* 2015;73:62–72.
62. Calhoun VD, Sui J. Multimodal fusion of brain imaging data: a key to finding the missing link(s) in complex mental illness. *Biol Psychiatry* 2016;1:230–44.
63. Marquand AF, Rezek I, Buitelaar J, et al. Understanding heterogeneity in clinical cohorts using normative models: beyond case control studies. *Biol Psychiatry* 2016;80: 552-61.